Effects of Thermomechanical Processing Conditions on the Morphology and Mechanical Properties of *Spirulina* Bioplastics

Hareesh Iyer

A thesis

submitted in partial fulfillment of the

requirements for the degree of

Master of Science

University of Washington

2022

Committee:

Eleftheria Roumeli

Navid Zobeiry

Program Authorized to Offer Degree:

Department of Materials Science and Engineering

University of Washington

Abstract

Effects of Thermomechanical Processing Conditions on the Morphology and

Mechanical Properties of Spirulina Bioplastics

Hareesh Iyer

Chair of the Supervisory Committee:

Assistant Professor Eleftheria Roumeli

Department of Materials Science and Engineering

The increasing consumption of non-degradable plastics and its harmful effects on the environment urgently call for the design and fabrication of degradable and renewably sourced materials. Recent studies have reported a mitigating strategy where materials derived from biological materials, or biomatter, are introduced as fillers in common plastic matrices, thus minimizing the use of non-renewable materials. For example, algae organisms, and more specifically *spirulina* microalgae, are a promising candidate for biomatter fillers as they can grow in a wide variety of aquatic environments and are already cultivated at industrial production rates as food supplements. However, the poor bonding between *spirulina* (and other plant-based biomatters) and common plastics often lead to the mechanical weakening of the produced biocomposites. The heavy use of chemical additives and multi-step processing necessary to circumvent these bonding obstacles have rendered the manufacturability of this filler-based strategy challenging.

In this thesis, we focus on pure bioplastics made almost exclusively of *spirulina*, where biomatter is not used as a filler but instead composes the bulk matrix of the fabricated materials. Upon hot-pressing, i.e., compression-molding under the given temperature and pressure conditions, *spirulina* powder can self-plasticize and get transformed into a bioplastic material which is strong, modifiable by common manufacturing techniques, and degrades in common soil. In this work, commercially acquired *spirulina* powder was hot-pressed under varying temperature, pressure and time conditions and the resulting bioplastics were mechanically tested in bending. Their morphology was studied via scanning electron microscopy (SEM), thus enabling us to draw connections between processing conditions, microstructure, and macroscopic mechanical properties. First, the effect of time in the compression molding process was studied. We observed that above a threshold of 5-minutes press time, the mechanical properties reached a plateau, with no significant changes in longer press times. Therefore, when studying the effects of pressure and temperature, the 5-minute press time was kept constant. By scanning a broad range of processing temperatures (60-160 °C) and pressure loads (2 – 35 kN), the produced *spirulina* bioplastics were found to span a wide range of mechanical properties and morphologies. At the lower end of the temperature/pressure conditions, a low bending strength of 1.2 MPa was measured, as the specimen remained in a loosely bonded powder form with intact and distinct cells still visible in the SEM. The strongest bioplastics were pressed at 140 °C and 7 kN and had a bending strength of 25.5 MPa. The SEM shows a completely different morphology, with a smooth fracture surface showing no distinguishable *spirulina* cells. At the higher end of the pressing conditions, thermal degradation initiation was observed, with a reduction in strength to 17.4 MPa.

In addition to pure-*spirulina* bioplastics, we also investigated the effects of introducing a plasticizer to further expand the attainable material properties. We used 1 - 30 wt% of a natural, plant derived plasticizer, sorbitol, which was compounded with the *spirulina* via twin-screw extrusion to create *spirulina*/sorbitol composites. The resulting powder was pressed using a given set of temperature, pressure and time conditions that were chosen to prevent the plasticizer from melting. For samples pressed at low temperature/pressure conditions, the addition of sorbitol showed strength increases of 2.4 times, elongation to break increases of 2.7 times, and toughness increases of 16 times. In addition to the morphological and mechanical properties, we used thermogravimetric analysis (TGA) to examine the thermal stability of powdered and pressed *spirulina* and conducted a soil degradation study to assess the biodegradability of our bioplastics.

Table of Contents

LIST OF FIGURES

LIST OF TABLES

ACKNOWLEDGEMENTS

First, I would like to thank my advisor, Prof. Eleftheria Roumeli, for convincing me to join her incredible group, inviting me to stay for my PhD, and above all for providing technical and emotional support throughout my journey towards achieving my Master's degree. I would also like to thank Prof. Navid Zobeiry for agreeing to be on my Master's thesis committee.

Dr. Bichlien Nguyen and Dr. Karin Strauss from Microsoft Research deserve special thanks for helping to provide career and scientific guidance for me throughout my time working on this project. Thank you to Microsoft Research for helping to fund this research as well.

Next, I would like to thank my lab members and former lab members for their friendship and help over the one and a half years that I've been in this group: Ian Campbell, Jeremy Fredricks, Paul Grandgeorge-Rognon, Mike Holden, Andrew Jimenez, Esther Law, Tim Liao, Meng-Yen Lin, Brandon Lou, and Mallory Parker. I am grateful to my friends Dylan Lawrence, Marek Moreno, Alex Narayanan, Colin Warnes, and Julia White for helping me stay grounded in the whirlwind of experiments and data that turned into this thesis.

Finally, and most importantly, I would like to thank my family for giving me inspiration and for supporting my desire to follow my research interests.

1. – Introduction

1.1 Effects of plastic pollution

World consumption of petrochemical-based plastics has been increasing around the world for decades, which has led to a significant problem of plastic pollution ending up in landfills and ocean environments [1]. As shown in Figure 1, the total amount of plastic produced by 2050 is predicted to be 33 billion tons, compared to 0.28 billion tons in 2012 [2]. Regions such as North America, Australia, Europe, and Japan consider petrochemically-derived polymers as generic solid waste, which allows for them to collect in landfills, waterways, and oceans.

Figure 1. The amount of plastic being used does not show any signs of slowing down. Image reproduced from [2].

The chemical stability of the polymers composing these common plastics, which makes them ubiquitous in numerous applications, also means that the plastics do not have the ability to degrade into constituent components. Instead, the plastics break into smaller pieces, termed microplastics, which can seep into food and water systems at all levels of the food chain, leading to health hazards throughout the environment [2]. As an alarming example, a recent study reported the presence of microplastics in human blood [3].

1.2 Sustainable solutions

The issue of plastic pollution has been known about for decades, and in that time some solutions have been developed. In Figure 2, we report common plastics sorted according to their source and biodegradability. In the top-left corner, conventionally produced polymers such as polypropylene (PP) and polyethylene (PE) are highlighted. The figure also shows that petrochemical polymers can be tailored to be biodegradable (such as polybutylene adipate terephthalate (PBAT)), which is a step toward solving the biodegradation problem, but not the petroleum sourcing problem with conventional polymers. Naturally derived polymers (bottom-right corner in Figure 2) can be produced from bacteria, plants, and even animals, but their biodegradability is not assured despite the natural source. Biobased, non-biodegradable polymers include perfluoroalkoxyl alkane (PFA) and biopolyethylene (Bio-PE). Polymers that are biobased and biodegradable, such as polylactic acid (PLA), show potential to reduce sourcing and biodegradation issues, as they are renewable and compostable [4, 5].

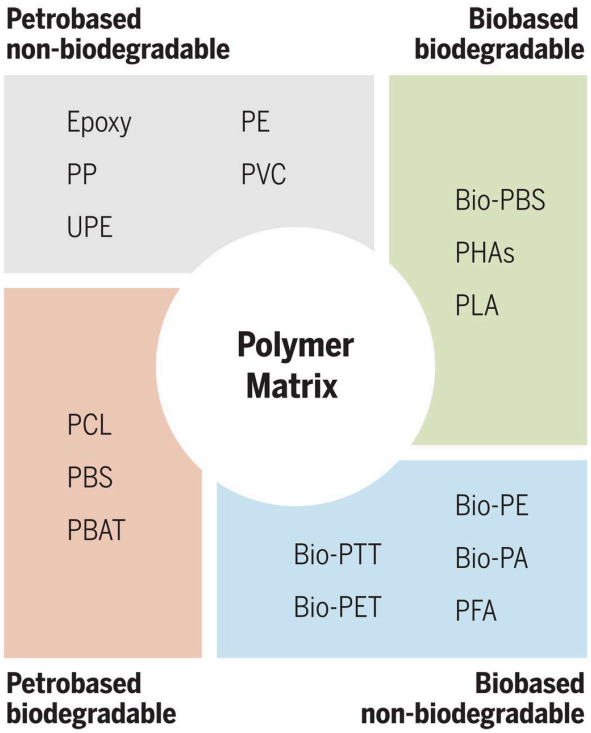

Figure 2. Some polymers are petroleum-derived but degradable, some are naturally derived but non-degradable, and others are in-between. Image is reproduced from [1].

One of the most commercially successful biodegradable thermoplastics [6], PLA is a polymer derived from corn or other similar starchy plants and is industrially compostable. Along with its relative ease of production, its renewable, natural resource base and compostability have made it widespread as a plastic for single-use items in modern society. However, PLA can only be composted in aerobic environments which can be achieved in industrial facilities, which most regions around the world are not equipped with.

Another solution to the plastic problem is to use lignocellulosic materials with minimal chemical processing. Cellulose is the most abundant natural polymer, made up of glucose units, and it provides the backbone for most plants as it is the main component in plant cell walls. The availability of this natural polymer makes it a desirable material to work with in creating biodegradable materials that can rival the mechanical properties of plastics [7]. Lignin is another dominant polymer component in cell walls, acting as a binder for cellulose with other polymer components while also providing rigidity and hydrophobicity. The combination of lignin and cellulose into a plastic material has been explored recently in literature, as shown in Figure 3, providing promising mechanical, thermal, and hydrophobic results [8, 9]. A key benefit to the use of lignocellulosic sources to make plastics or bioplastics is that waste materials can be used instead of being burned, which is a typical solution to waste natural fibers that releases carbon dioxide into the environment.

Figure 3. While lignocellulosic materials are promising, one drawback is the chemical processing required to produce many of them. Image is reproduced from [8].

One drawback from lignocellulosic materials is the amount of chemical modification often required to produce useful materials [10]. Functionalization of the cellulose surface is often performed to ensure compatibility with other materials, or to improve hydrophobicity or barrier properties [11]. Other chemical processes may need to be employed to separate the lignin and cellulose from each other, as well as from the other molecules in the plant matter. The production and discarding of these chemicals increase the environmental impact of producing these materials, which makes the argument to convert to bioplastics more difficult when comparing them to traditional polymers that are incredibly cheap and useful.

1.3 Benefits of using algal biomatter

Materials produced from algae-based sources have been reported as alternatives to lignocellulosic bioplastics [12]. Similarly to corn being considered a valuable feedstock for PLA, algae is a promising feedstock for bio-based plastics. Like corn, there is a potential for large amounts of waste algae. As the benefits of algae as a feed for livestock as well as a supplement to human diets is increasingly studied, the number of algae farms is set to increase. Algae have fast

growth rates and can grow in a wide variety of aquatic environments [13]. This environmental resilience provides promise for algae to be grown locally to where it is developed into a bioplastic material, reducing transportation emissions and costs. In addition, algae as a photosynthetic organism can serve as a carbon sink which allows it to improve the environment that it is grown in. As the call to action to slow climate change increases, the development of algae farms for environmental reasons is likely to increase. With increased algal growth, and due to the fast growth rate of algae, there is likely to be a lot of waste produced from such algae farms. Therefore, it is important to be able to take that waste and turn it into useful products.

Only one bioplastic made from pure algae has been reported, with *spirulina* and *chlorella* algae being used to create dog bones with tensile strengths of 3.0 and 5.7 MPa, respectively [14]. Algae and polymer blends, where algae is introduced as a filler, have been commonly studied, with bioplastics having been made from combinations with polyvinyl alcohol (PVA) [15] and polyethylene (PE) [14, 16], with glycerol as a compatibilizer between the two materials. Algae has also been used as a source of starch production [13]. Even with these exciting uses of alternative material sources, there is still a lot of room to study the use of pure, whole algae cells in making useful bioplastics.

1.4 Objectives

Despite the promising ideas that algae and its potential bioplastics provide, the reality is that the development of bioplastics still has a way to go before moving from the conceptual space to the commercial space. The goal of this study was to examine the effects of processing parameters on the algal species *spirulina* subjected to compression molding, as well as the effects of introducing a natural plasticizer additive to change its mechanical properties. We followed a wasteless manufacturing process, in that the entire microorganism was utilized without extraction or chemical modification processes, and water was the only solvent used. Commercially viable

manufacturing processes were employed, such as compression molding and twin-screw extrusion, to demonstrate the ability of algae cells to be made with currently available techniques.

Spirulina was chosen as the algae because of its abundance and commercial use as a dietary supplement, which means that it is already an easily available base material. Similarly, sorbitol is a widely available natural polyol, making it a low-impact additive for the bioplastic. Three-point bending was used to mechanically characterize the specimens, while scanning electron microscopy (SEM) was used to examine the morphological changes caused by the different processing and additive parameters. Thermogravimetric analysis (TGA) was used to examine the thermal stability, and a biodegradation study was used to compare the ability for algae-based bioplastics to degrade when compared to another natural material (banana peel was used as a positive control) and a commercially available, naturally derived non-soil degradable polymer (PLA was used as a negative control).

Chapter 2 – Material Methods

2.1 Algae and sorbitol material procurement

Spirulina algae cells were procured from Nuts.com as Organic Spirulina. Sorbitol was purchased from Sigma Aldrich.

2.2 Compression molding using a hot press

A hot press was used to apply temperature and a pressing force to the powders to produce plasticized specimens. The hot press was a TMAX-SYP-600 from TMAXCN.

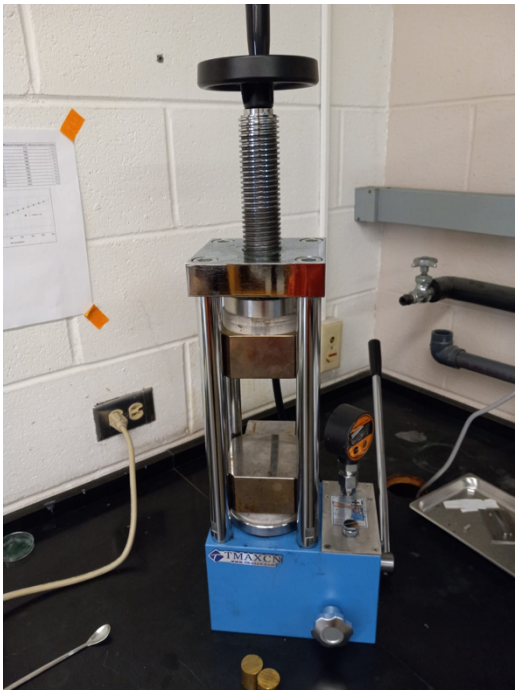

Figure 4. TMAX-SYP-600 hot press used to produce samples for this experiment.

As shown in Figure 4, the hot press has two platens that are heated. The temperature is set by two control boxes, but a thermocouple was used to ensure the platens were at the correct temperature. A calibration was performed to determine what to set the temperature of the hot press in order to achieve the desired temperature. Figure 5 shows the linear trend line that was used to determine hot press set temperatures, with values from Table 1 showing the set and recorded

temperatures. Equation 1 shows the linear equation that was used for approximating the real temperature based on the temperature set on the hot press.

Table 1. Temperatures set on the hot press versus the temperature measured by the thermocouple on the platens.

Set Temperature (°C)	Measured Temperature (°C)
48.5	60
69	81
88	100
112	120
129	140
150	160

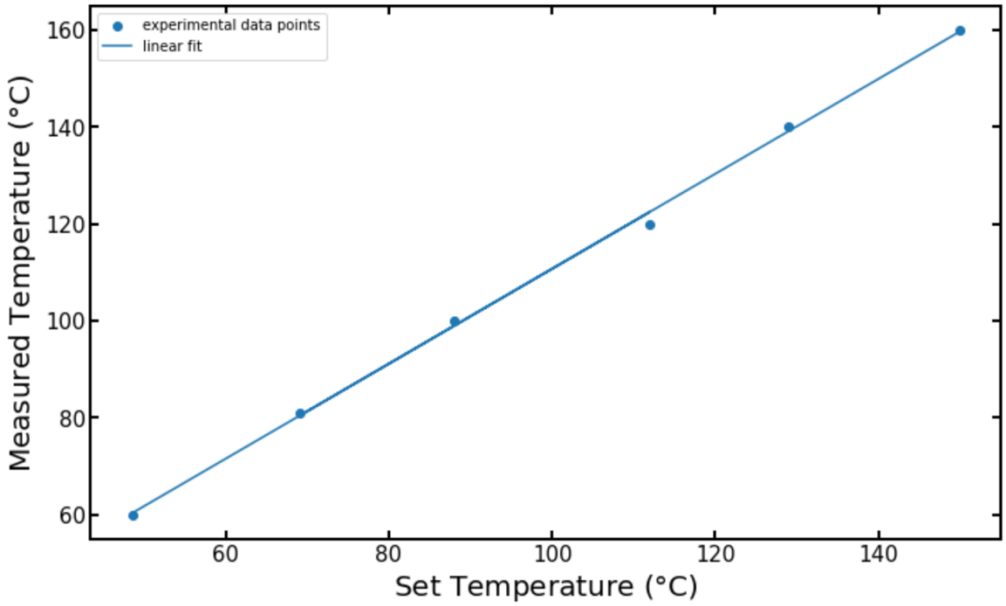

Figure 5. Measured temperature from the thermocouple vs set temperature on the hot press with a linear fit applied.

$$Measured\ Temperature = 0.979 * Set\ Temperature + 12.9 \quad (1)$$

To press the samples, a three-part mold was designed and machined. The material for the mold was stainless steel, which was chosen for increased durability over the cheaper aluminum, a quality that was important to consider when looking at the number of samples that were required for this study. An exploded view of the 3D model for this mold is shown in Figure 6, created using Autodesk Fusion 360.

Figure 6. Exploded view of the 3-piece mold assembly.

Because of the low thermal conductivity of stainless steel, the mold pieces were heated on a hot plate to approximately the same temperature as the hot press. This pre-heating step ensured that the powder would spend the vast majority of its time in the mold at the intended temperature. The pure *spirulina* specimens were fabricated by placing the short bottom piece of the mold in the slot in the middle piece of the mold. The resulting cavity was then filled with one gram of *spirulina* powder, making sure that the powder is evenly spread out throughout the mold. Finally, the tall top piece was inserted into the cavity, compressing the powder between the top and bottom pieces. The filled mold assembly was then placed between the hot plate platens set to the proper temperature, the platens were tightened around the mold, and the pressure reading on the hot press was set to the appropriate reading based on the required pressing force. Once the pressure was reached, a timer was started, and the pressure was held for the entire duration. The molds were allowed to cool to handling temperatures before the specimens were removed. While cooling, the mold was placed between aluminum blocks that acted as heat sinks as well as weights to ensure the specimens remained flat while cooling.

While the hot press reads out a pressure value when pressing samples, that pressure is not transferrable to hot pressing machines of different sizes. Therefore, a desired pressing force was used, and converted to an appropriate pressure reading from the hot press. The piston diameter in

the hot press was 95 mm in diameter. This diameter was used to convert the desired pressing force to a pressure reading on the hot press, as displayed in Table 2.

Table 2. Pressing force conversions to pressure readings on the hot press.

Pressing Force (kN)	Hot Press Pressure (MPa)
2	0.28
7	0.99
20	2.82
35	4.94

2.2.1 Time sweep

The hot press has three variables that can be adjusted during the production of the specimens used in this study: temperature, pressing force (also referred to as a pressure), and time spent at that pressure. It is difficult to visualize the effects of three variables without a freely moving 3D plot, so one of the variables was isolated. Through preliminary testing, it was predicted that time was likely to have the least effect on the degree of plasticization of the specimens. Therefore, time was chosen as a variable to isolate and change, while keeping the temperature and pressure constant. This way, if there was a minimum time required for full plasticization (as characterized by flexural strength), it could be used as the unchanging variable when examining the other two parameters.

A temperature of 120 °C and a pressing force of 7 kN were used as constants because this set of conditions was a good middle ground for the various conditions that would be used in the temperature/pressure matrix, and it was likely to produce robust, testable samples at low pressing times. The samples were pressed for 0, 10, 30, 60, 300, 600, and 1800 seconds. For the 0 second pressing condition, the pressure valve on the hot press was released as soon as the desired pressing force was achieved. Based on this study, a pressing time of 5 minutes was chosen to be held constant for future *spirulina* tests.

2.2.2 Temperature/Pressure sweep

With a constant time of 5 minutes for each press, the temperature and pressure could be varied. A set of temperatures ranging from 60 °C to 160 °C and a set of pressing forces from 2 kN to 35 kN were chosen. The maximum temperature of 160 °C was chosen to get close to the degradation temperature of *spirulina* based on TGA data. The minimum temperature was chosen based on prior tests that showed great difficulty in creating testable samples at lower temperatures. The maximum pressing force was chosen as the maximum that the stainless-steel mold could withstand before deforming, as well as to reduce the risk of *spirulina* flowing out of the mold due to plasticization. Based on these sets of temperatures and pressures, 24 trials were developed, as outlined in Table 3. Trials 1 and 5 were not able to produce testable samples, so data is only shown for 22 trials in the subsequent sections. As previously mentioned, all runs had a pressing time of 5 minutes.

Table 3. Hot pressing parameters for the temperature/pressure matrix.

Run	Temperature (°C)	Pressing Force (kN)
1	60	2
2	60	7
3	60	20
4	60	35
5	80	2
6	80	7
7	80	20
8	80	35
9	100	2
10	100	7

11	100	20
12	100	35
13	120	2
14	120	7
15	120	20
16	120	35
17	140	2
18	140	7
19	140	20
20	140	35
21	160	2
22	160	7
23	160	20
24	160	35

2.3 Extrusion mixing

To create the *spirulina*/sorbitol composites, proper mixing of the two powders was very important, especially for low sorbitol concentration samples. To accomplish this mixing, the two powders were first weighed out into a single tube. The tube was then mixed using the Analog Vortex Mixer, produced by VWR in Radnor, PA, USA. The mixer was used for approximately 5 seconds at maximum power. The material was then fed through a Scientific Process 11 Twin-Screw Extruder, made by Thermo Fisher in Waltham, MA, USA. The extrusion profile had a

temperature of 90 °C at all heating zones, and a screw rotation rate of 40 rotations per minute (RPM) was used.

Figure 7. The extruder that was used to homogenize the *spirulina* and sorbitol powders.

As shown in Figure 7, the extruder has a feeder on the right, where the mixed powder was fed into. Typically, this extruder has a 2 mm diameter die on the left end of the machine. However, for the purposes of this study, the die was removed, as a mixed powder was all that was necessary. While the high sorbitol concentrations can lead to the production of a filament using this die, low sorbitol concentrations do not produce filaments, so using the die would not have been tenable for all trials in this experiment.

Once a homogenous powder was produced by the extruder, the powder was loaded into molds and pressed as outlined in the previous section. However, the pressing conditions were kept constant to examine the effect of changing sorbitol concentrations on the specimen. Table 4 shows the pressing conditions and sorbitol concentrations used.

Table 4. *Spirulina*/sorbitol specimen production parameters.

Trial #	Sorbitol Concentration (wt. %)
1	0

2	1
3	5
4	10
5	30
All samples were pressed at 80 °C/7 kN/1 minute	

In Chapter 3, this paper demonstrates that the chosen pressing conditions for the *spirulina*/sorbitol production do not produce fully plasticized samples in pure *spirulina*, rather it would produce a sample that is held together mostly through powder-packing. The reason for this is that at higher pressing conditions, the sorbitol would melt out of the mold, carrying the *spirulina* with it. Over time, this would lead to deformation of the molds, and it would produce untestable samples.

2.4 Analysis

2.4.1 Mechanical testing

After production, each sample was labeled and placed in a desiccation chamber for 24 hours. Water has a well-known plasticizing effect on biopolymers, hence the importance of the desiccation step [17]. Once a specimen had reached at least 24 hours of desiccation, their thicknesses, widths, and masses were measured.

Three-point bending was chosen as the mechanical analysis method of choice. Tensile testing was attempted first, but it was very difficult to produce films of *spirulina* at uniform thicknesses, and these films were not able to be gripped in the tensile testing apparatus. Instead, the AGS-X (10 kN) test frame, made by Shimadzu Scientific Instruments in Columbia, MD, USA, was used in a three-point bending configuration. All samples were tested at a 0.5% strain rate. The stress on a sample in three-point bending is calculated using **Equation 2**

$$\sigma_f = \frac{3FL}{2bd^2}, \quad (2)$$

where σ_f is the flexural stress at the outer surface at the midspan of the beam, F is the load at a point on the load-displacement curve, L is the support span of the test setup, b is the width of the specimen, and d is the depth of the specimen. This equation is appropriate for three-point bend specimens with a rectangular cross-section, which was the case with the samples used in this study. Figure 8 shows a picture of the test setup that was used for this experiment.

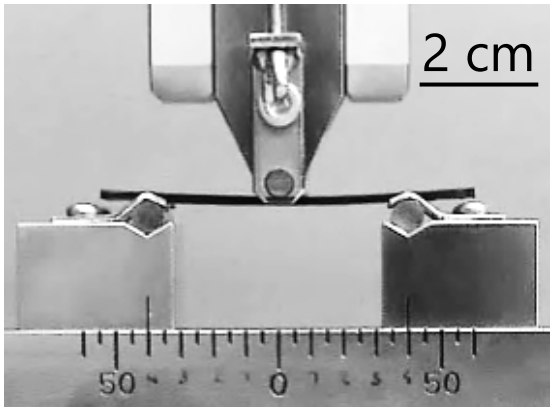

Figure 8. Three-point bend setup.

The support span for these tests were either 40 mm or 20 mm. Full specimens were tested at the 40 mm span length, with the sample breaking in half. Each half was then tested on the 20 mm support span. There was no significant difference observed in the mechanical properties between testing the full specimens and the half specimens, so the procedure was deemed adequate. Three specimens were produced for each trial, giving nine samples total for each trial, when including the number of half-specimens tested on the 20 mm span.

2.4.2 Nanoindentation

Nanoindentation is a type of mechanical test that uses a micron-scale tip to locally test the mechanical properties of a material. It is commonly used to measure hardness, but it can also be used to calculate a reduced modulus to characterize the stiffness. **Equation 3** shows the equation used to calculate the stiffness during a nanoindentation test.

$$E_r = \frac{1}{\beta}\frac{\sqrt{\pi}}{2}\frac{S}{\sqrt{A_p(h_c)}} \quad (3)$$

E_r is the reduced Young's modulus, β is a geometrical constant for the specific type of indenter, S is the stiffness as measured by the slope of the load-displacement curve at the point of unloading, and $A_p(h_c)$ is a fitting polynomial specific to the type of indenter being used. For these tests, a Berkovich tip was used. The reduced modulus was used in this study to confirm the trends of flexural modulus produced by the three-point bend testing. The nanoindentation machine used for this experiment was an FT-MTA03 produced my Femto Tools.

2.4.3 Scanning Electron Microscopy

Scanning Electron Microscopy (SEM) was used to observe morphological changes at the sub-microscopic level. Samples were sputter coated with approximately 4 nm of platinum on an EM ACE600, produced by Leica Microsystems. The SEM imaging was done on an Apreo VP, made by ThermoFisher Scientific.

2.4.4 Thermogravimetric Analysis

Thermogravimetric Analysis (TGA) allows for the measuring of the change in weight of a sample when subjected to a selected temperature treatment. It is comprised of placing the sample in a non-reactive crucible with a high melting point, which is then loaded into a furnace. The crucible hangs from a wire that is connected to a scale, which measures the change in weight. A thermocouple is situated next to the sample to measure the temperature. Thermogravimetric analysis is used to determine the thermal stability of materials, as well as examining water loss in hydrophilic materials or mass gain for oxidizing materials. The TGA was performed on a Discovery TGA 550, from TA Instruments in New Castle, DE, USA. Approximately 13.421 ± 4.277 mg of each sample was placed in a platinum sample pan and subjected to heating from room temperature to 1000 °C at a heating rate of 10 °C/min and in a nitrogen gas flow of 40 μL/min.

2.4.5 Differential Scanning Calorimetry

Differential Scanning Calorimetry (DSC) is used to study thermal events that materials undergo during heating and cooling cycles. A sample and reference crucible are placed in a chamber that is equipped with temperature sensors. The chamber is heated or cooled according to the set program and the difference in temperature between the reference and sample crucibles is measured. An integral of the change in temperature curve is used to calculate the changes in heat flow. When a sample undergoes a thermal event, the heat flow will either increase or decrease depending on if the thermal event is exothermic or endothermic.

Sorbitol was studied using a Discovery 2500 DSC from TA Instruments in New Castle, DE, USA. Hermetically sealed TZero aluminum pans were used to hold the sample and as a reference. Two heating and cooling cycles each were done at rates of 10 °C/min, with isothermal holds of 1 minute between each cycle. The DSC experiment was run from -75 °C to 200 °C.

2.4.6 Biodegradation

An ongoing biodegradation study was used to gather data for this experiment. The biodegradation study was at week 6 at the time of the writing of this thesis. Samples of different materials, including a banana peel, PLA, and a *spirulina* bioplastic, with approximately equal surface area, were buried under gardening soil. The soil was regularly watered to ensure a damp environment. Every two weeks, the samples were dug up and their change in weight from the previous measurement was recorded. PLA was chosen because it is a commonly used plastic that is considered compostable. A banana peel is a commonly available, purely natural material that degrades on a kitchen counter, let alone buried in soil. These materials were used as comparison points to give the degradability of the *spirulina* bioplastics context.

Chapter 3 – Results and Discussion

3.1 Mechanical and Morphological Analysis of *Spirulina*

3.1.1 Density Changes

The first step of the mechanical testing process was to measure the mass, length, width, and height of each specimen so that the density could be calculated. Based on the design of the mold, an approximation of the density had to be made. As can be seen in Figure 9, the mold has an obround slot shape, but the ends of the slot are not perfect semicircles. Instead, each end is two arcs of radius 3.5 mm connected by a short line of 1.0 mm. This ideal case is never achieved by the actual pressed samples, and it is difficult to measure the radius of the arcs and distance between them in a real sample. In order to complete the density calculation, an assumption that the 1 mm separation was true for all parts was used.

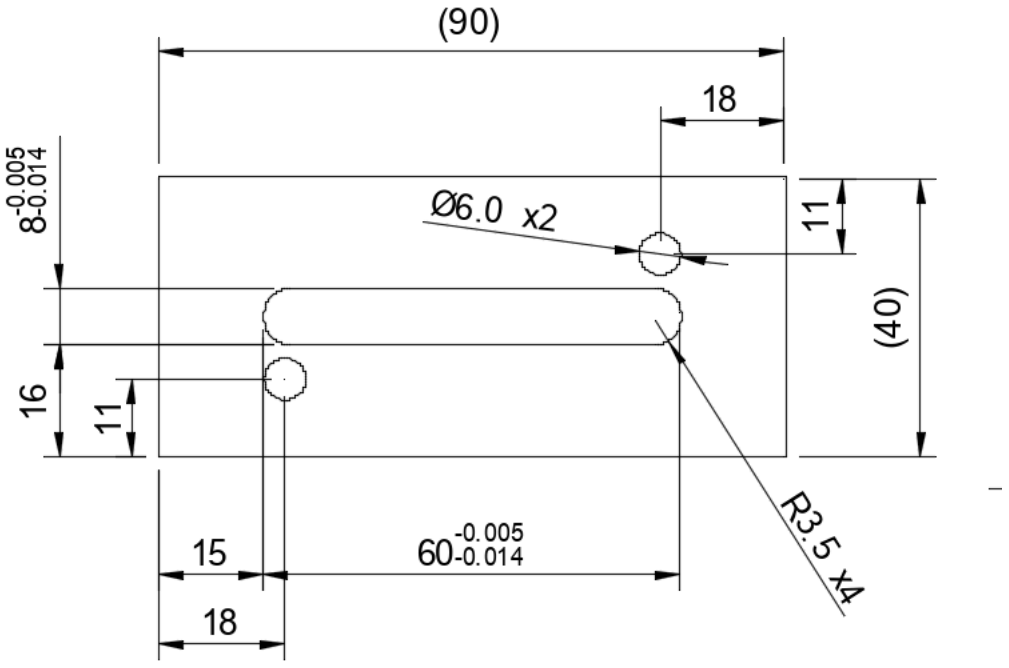

Figure 9. 2D drawing of the middle piece of the 3-piece mold.

Density was plotted versus temperature and pressing force to examine any relationships between the three variables, as shown in Figure 10. In the Density vs Temperature plot on the left,

it is generally observed that as temperature increases, the density of specimens approaches approximately 1.2 g/cm^3. At lower temperatures, the scatter in densities can be explained by the lack of plasticization in the specimens. The materials are a packed powder with loose bonding rather than a plastic piece, so the force at which the samples are pressed has a higher impact on the density. In the Density vs Pressing Force plot on the right, a similar trend is observed. Density generally does not change significantly as pressing force is increased except for at the lowest of temperatures, while the densities see greater change from temperature line to temperature line.

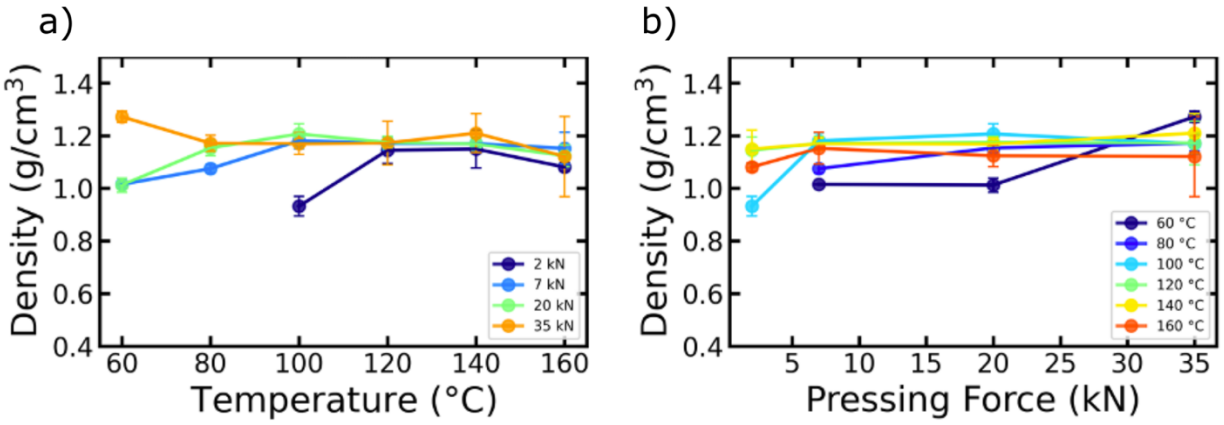

Figure 10. a) Density vs Temperature at different pressures. b) Density vs pressing force at different temperatures.

The last part of the density analysis was analyzing the density vs the strength of the materials. Figure 11 shows a plot of error bars in both the strength and the density axes, with the center of the error bars being the average value coordinate. This plot shows the large amount of grouping around the 1.1 to 1.2 g/cm^3 density values, with strengths varying significantly in that range. Meanwhile, some samples are significantly less dense, with one outlier being more dense but also less strong. All this data indicates that it is not merely powder packing that is affecting the strength of these materials, there is an actual change going on that leads to a plasticized part that can be tuned higher or lower in strength and toughness based on hot pressing parameters.

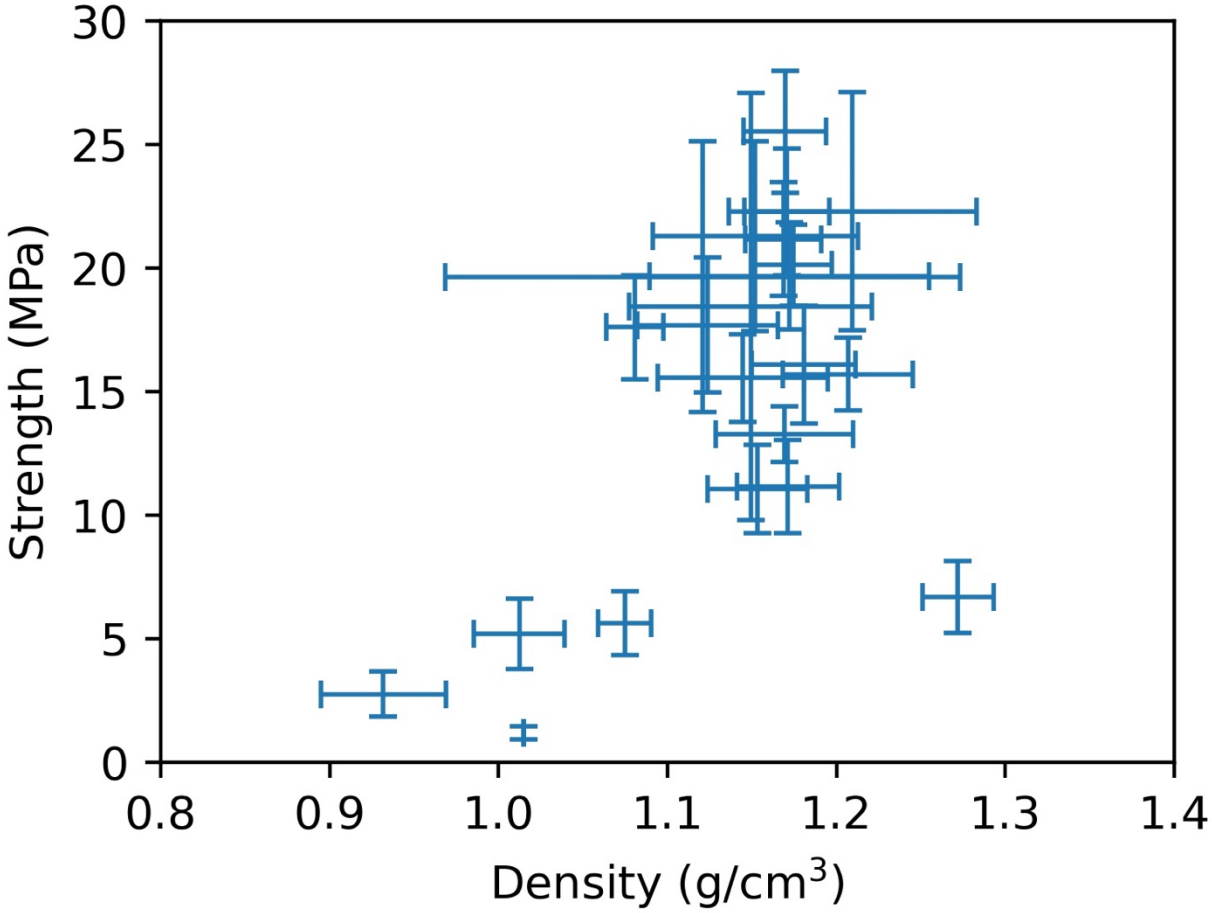

Figure 11. Strength vs density, with error bars showing the standard deviation in both axes.

3.1.2 Mechanical Properties

The hot press has three variables that can be changed to affect the manufacturing process: temperature, pressure, and time. To determine the effects of these three variables on the mechanical properties of the bioplastics, one variable was isolated and then held constant so that only two variables needed to be compared to each other. Time was chosen as the variable to hold constant. In Figure 12, a plot of strength vs time was created, with temperature and pressing force being held at a constant 120 °C and 7 kN, with time being variable from 0 to 30 minutes. These constant values were chosen based on prior experience with hot pressing indicating that testable samples would be produced even at the 0 second pressing condition. It is clear from the plot that a plateau in strength is reached between the 60 and 300 second pressing conditions, and further

pressing does not have a significant impact on the bending strength. The 300 second (5 minute) condition was chosen for subsequent tests because of its presence further along the saturation point, its low standard deviation in measured strength values, and to ensure comparisons with other bioplastics produced in our lab that are also pressed for the same time.

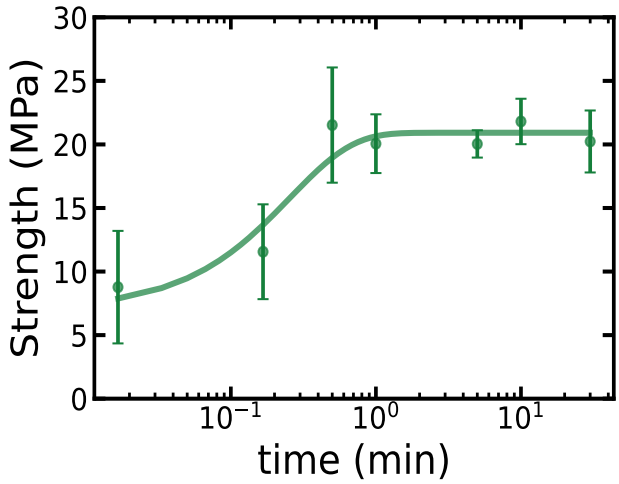

Figure 12. Strength of samples vs the time that they were pressed at. A plateau in strength is observed at approximately 5 minutes.

With a pressing time of 5 minutes to hold constant, the next set of experiments could be run to compare the effects of pressure and temperature on *spirulina* plastics. From the "lowest" pressing conditions to the "highest" pressing conditions, a general trend of increasing modulus was found, as shown in Figure 13.

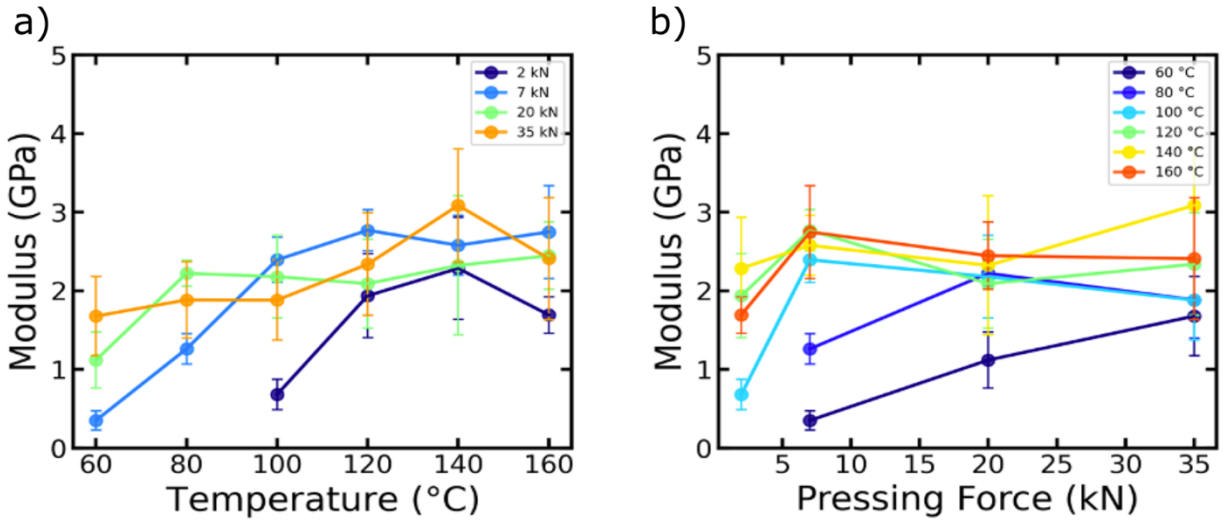

Figure 13. a) Flexural modulus vs temperatures at different pressures. b) Flexural modulus vs pressure at different temperatures.

Specifically, for the lowest pressure load (2 kN) a substantial increase in elastic modulus (from 0.68 ± 0.19 to 2.04 ± 0.47 GPa) was found as the temperature increased from 100 to 120 °C, which was maintained for the 140 °C and was slightly reduced (to 1.69 ± 0.23 GPa) at 160 °C. This significant increase – plateau – decrease trend was only observed to that extent at the minimum pressure conditions (2 kN) indicating that at this low pressure condition a temperature of 120-140 °C is required for the samples to reach the maximum elastic modulus. At lower temperatures the loose packing results in non-well-bonded bioplastics, while at maximum temperature thermal degradation initiation may be negatively affecting the sample performance. At a higher pressing load of 7 kN we observe the same substantial increase in modulus (from 0.35 ± 0.12 to 2.39 ± 0.29 GPa) with temperature increasing from 60 to 100 °C. Then the modulus plateaus and does not decrease at the maximum tested temperature of 160 °C. Similar modulus fluctuations exist but are smaller at a higher pressing load of 20 kN. A small increase (from 1.18 ± 0.31 to 2.22 ± 0.16 GPa) is observed when temperature increases from 60 to 80 °C and a plateau is reached above that threshold. In the maximum pressure loads of 35 kN the plateau is obtained even at 60 °C but the larger deviations for each sample indicate that the degree of uniformity in the samples is more variable than in any other pressing condition. Overall, we can conclude that the temperature threshold to achieve a bulk material varies significantly with the choice of applied pressure in the compression molding process. Low pressures shift the required temperature threshold to higher values while higher pressures reduce that temperature threshold. Yet the maximum tested pressure clearly is preventing homogenous sample formation as the error bars are significantly higher in these conditions. The maximum average modulus of 3.1 GPa was achieved at 35 kN and 140 °C. The minimum modulus was achieved at 7 kN and 60 °C.

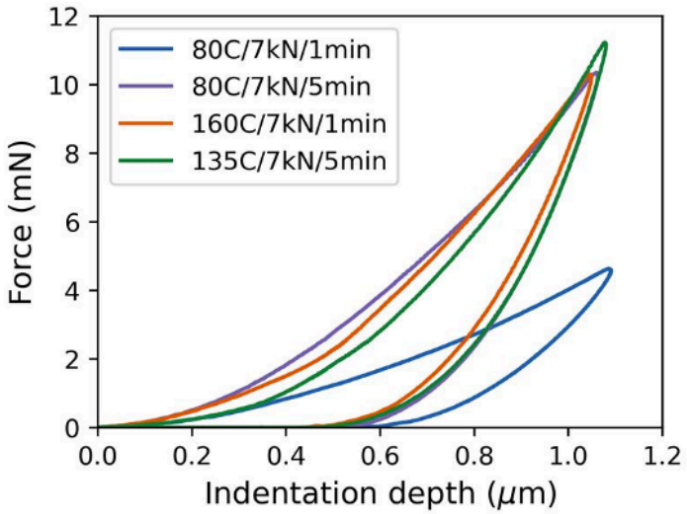

Figure 14. Loading and unloading curves procured from nanoindentation tests.

Representative loading and unloading curves from the nanoindentation measurements are shown in Figure 14. The reduced modulus was calculated using the slope of the unloading curve at maximum displacement along with the projected area of contact of the nanoindentation tip. This graph shows how poorly the material performs when the cells are being packed together without any plasticization occurring.

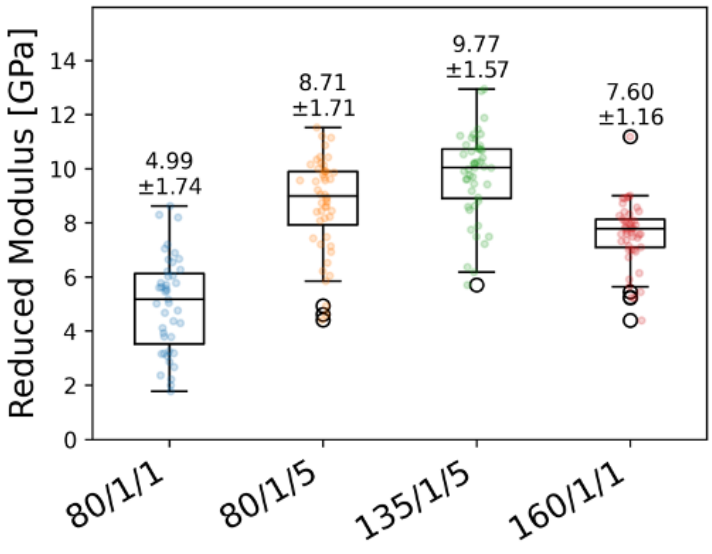

Figure 15. Nanoindentation data showing the reduced elastic modulus for various pressing conditions.

Figure 15 shows nanoindentation data for a set of samples deemed to be representative of the pressing samples, with the pressing conditions being listed as Temperature (°C)/Hot Press

Pressure (MPa)/Time (minutes). This figure shows the reduced modulus measured for each sample, with a "weak" sample at 80/1/1, two relatively strong samples in the middle, and a sample in the degradation temperature region at 160/1/1. The nanoindentation data corroborates the trend that is seen in Figure 13, with stiffness increasing with the intensity of the pressing conditions and dropping once the material starts to degrade.

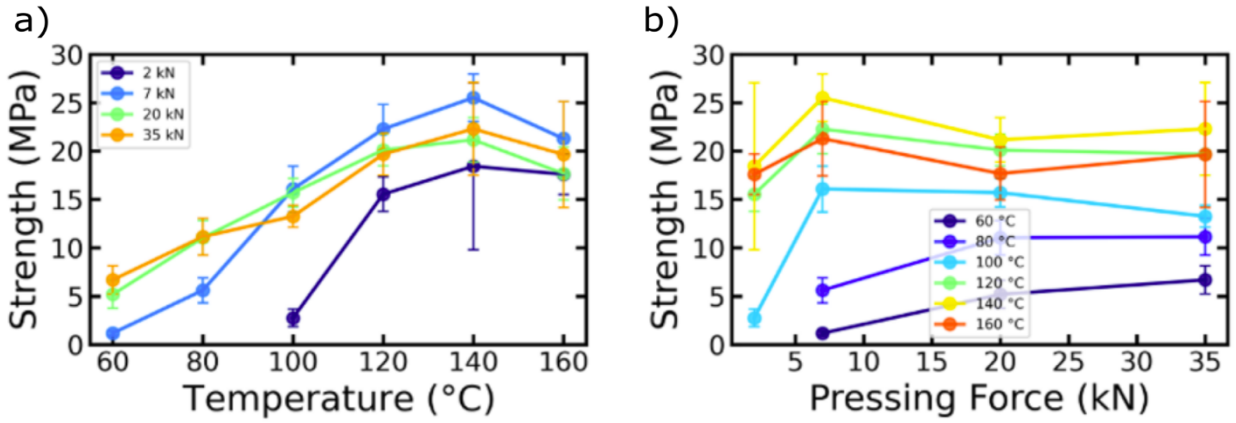

Figure 16. a) Flexural strength vs temperature at different pressures. b) Flexural strength vs pressing force at various temperatures.

Clearer trends are seen in the flexural strength of the *spirulina* specimens. Figure 16 shows the strengths of the tested specimens versus temperature on the left and versus pressing force on the right. A clear relationship between temperature and strength is seen in the temperature plot. As temperature is increased, strength is increased, until the degradation temperature is approached and strength trends downward.

According to Figure 16a, at the lowest pressing force of 2 kN there is a significant jump in flexural strength as the temperature increases from 100 to 120 °C (from 2.75 ± 0.90 to 15.54 ± 1.78 MPa), at which point a plateau is reached in strength. At a pressing force of 7 kN, the strength increases from 1.17 ± 0.27 MPa to 25.52 ± 2.47 MPa. The strength then drops to 21.28 ± 3.85 MPa when pressed at 160 °C, which may indicate the onset of degradation, although the overlap in error bars between those two temperatures makes that claim unsubstantiated. At 20 and 35 kN pressing forces, the low temperature strengths were higher than at the lower pressing forces

(5.18 ± 1.43 MPa and 6.68 ± 1.46 MPa, respectively), but they still see significant increases at 120 °C, at which point the strengths plateau at 20.10 ± 1.63 and 19.67 ± 2.17 MPa, respectively. Figure 16b clearly shows that a pressing temperature of 140 °C consistently produces higher average flexural strengths, while 160 °C generally produces lower average strengths than at 120 and 140 °C, again most likely because of the onset of degradation. The maximum strength of 25.5 MPa is reached at pressing conditions of 140 °C and 7 kN. While the degradation temperature can explain the downward trend of the data after 140 °C, it is also noticed that the 7 kN pressing condition produced higher strengths than the higher pressing force conditions. This may be explained by the observation that higher pressing conditions caused so much plasticity in the *spirulina* at higher temperatures that the material flowed out of the gaps in the mold, leading to thinner, less easily manufacturable parts. The demolding process for these specimens was difficult as the specimens ended up being rather fragile. 7 kN appears to be an acceptable compromise between having enough force to get a high strength value out of the material, but not so strong to disrupt the manufacturing process.

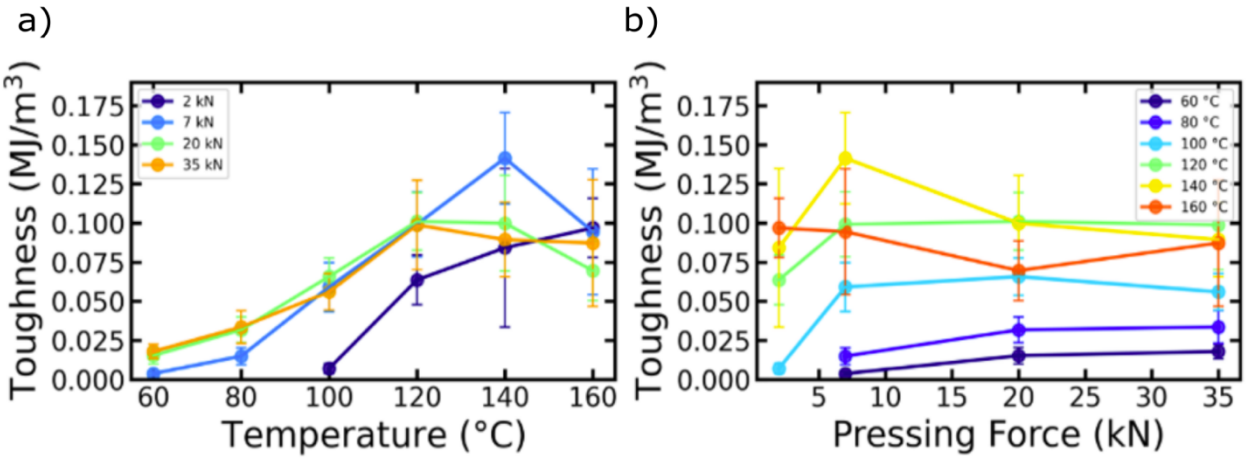

Figure 17. a) Toughness vs temperature at various pressing forces. b) Toughness vs pressing force at various temperatures.

The toughness of the specimens was similarly plotted against temperature and pressure in Figure 17. The toughness plots show almost the same trends as the strength plots. At the lowest

pressing force of 2 kN, there is again a significant jump in toughness from 100 to 120 °C, from 0.01 ± 0.00 to 0.06 ± 0.02 MJ/m^3, and it continues to increase up to 0.10 ± 0.02 MJ/m^3. At 7 kN, the toughness at 60 °C is essentially zero, while it climbs up to 0.14 ± 0.03 MJ/m^3 at 140 °C. It then sharply decreases to 0.09 ± 0.04 MJ/m^3 at 160 °C. At 20 kN, the toughness increases from 0.02 ± 0.01 MJ/m^3 at 60 °C to 0.10 ± 0.02 MJ/m^3 at 120 °C, and decreases to 0.07 ± 0.02 MJ/m^3 at 160 °C. At 35 kN, the pressing force increases from 0.02 ± 0.00 MJ/m^3 at 60 °C to 0.10 ± 0.03 MJ/m^3 at 120 °C, at which point it reaches a plateau in toughness. The similar trends shown in the strength and toughness plots indicate that, on average, the shapes of the stress strain curves are not very different from each other, and that can indeed be seen from Figure 18. The elongation to break was not significantly different across the hot-pressing conditions. The stress strain curves shown in Figure 18 indicate purely brittle failure, although there is ambiguity for the 60 °C samples, which again were mostly packed powder rather than a plastic material.

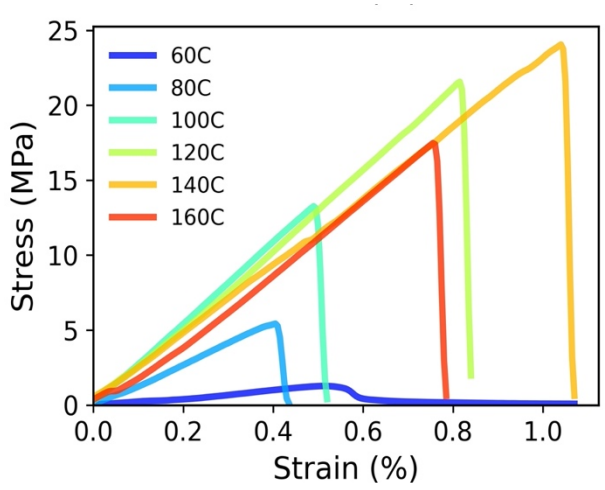

Figure 18. Representative stress-strain curves for the pure *spirulina* bioplastics.

3.1.3 Morphological Changes

Along with the mechanical property changes, morphological changes were observed at the microscopic level. As stated before, the *spirulina* starts as particles of dried out, deceased *spirulina* cells. With weak or no plasticization, the material ends up looking as shown in Figure

19. Parts of cells are still visible, and there are voids present in the final material. These voids are due to a lack of plasticization, but it is unclear if they are produced from the fracture mechanics of the material or from the poor packing of the powder at these low pressing conditions.

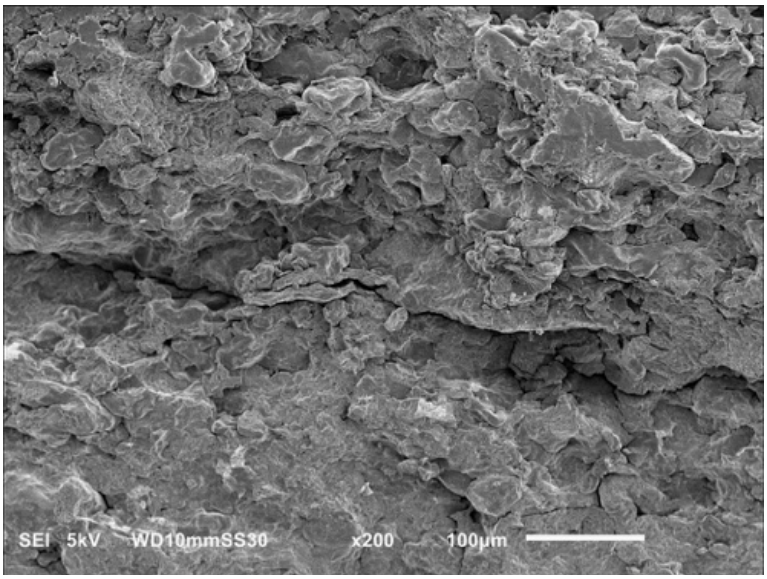

Figure 19. SEM image of a non-plasticized *spirulina* sample.

In contrast, Figure 20 shows the fracture surface of a fully plasticized sample at the same magnification. The sample appears smoothed out, and there are no individual cells visible. Much smaller cracks are visible, most likely from the fracturing rather than for powder-packing reasons.

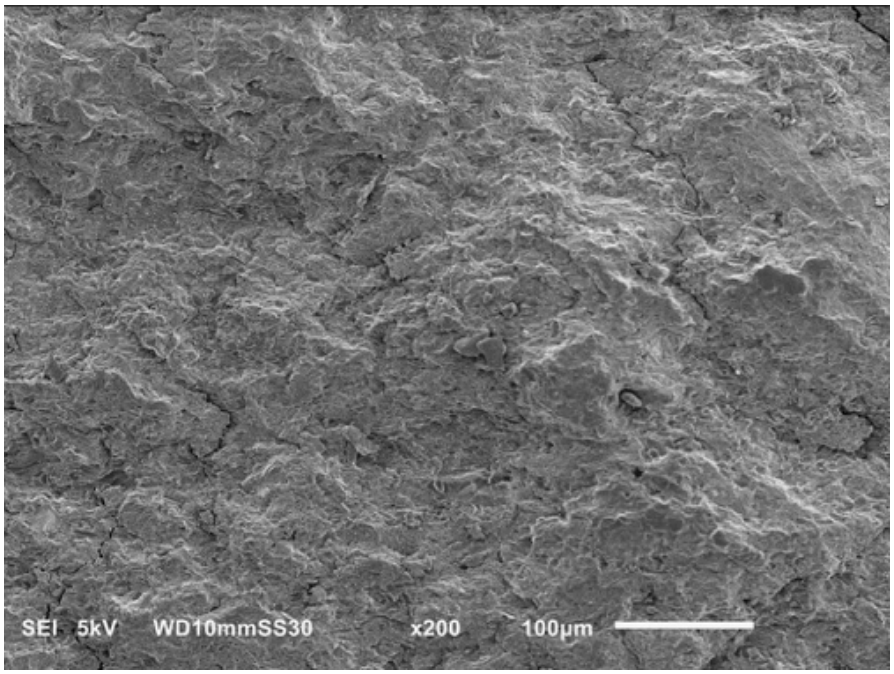

Figure 20. SEM imaging of a fully plasticized *spirulina* sample.

The biggest takeaway from Figures 19 and 20 is that the material has completely changed morphology. This is visible at the macro scale as well, as can be seen in the next two figures.

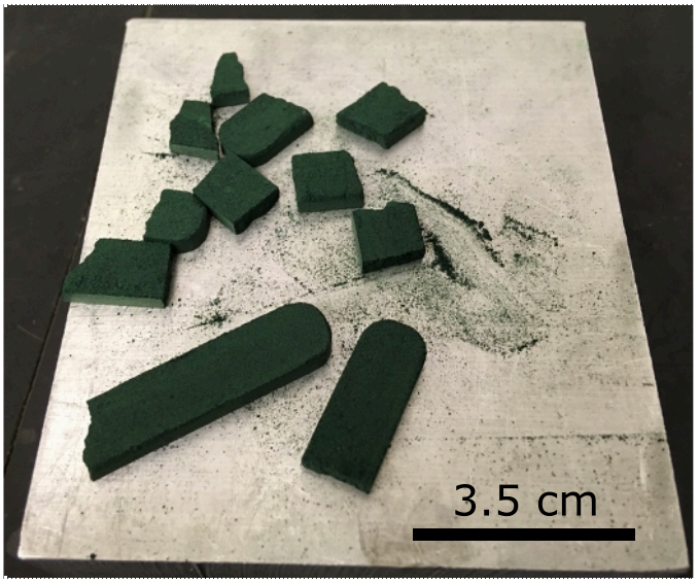

Figure 21. Unplasticized *spirulina* specimens.

Figure 21 shows a group of poorly plasticized specimens, where the properties come from powder packing rather than any real change in the material. The pieces shed powder just from touching or moving them, and they fell apart during normal handling. In comparison, Figure 22

shows a fully plasticized specimen. It is smooth like many commercial plastics and reflects light very well with a polished surface.

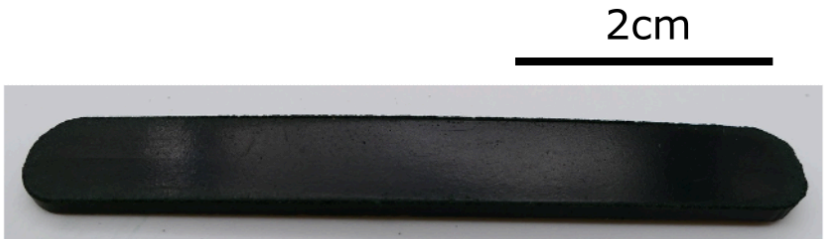

Figure 22. Fully plasticized *spirulina* specimen.

A strong indication that plasticization is happening is the way the surface behaves at extreme pressing conditions. During tests where time was variable and temperature was extreme, short pressing times would lead to bubbles forming in the surface of the specimen, as shown in Figure 23. This behavior is most likely due to the top layer of the specimen plasticizing and becoming impermeable to water while the underlying powder is still evaporating out humidity, leading to bubbles forming in the plasticized layer.

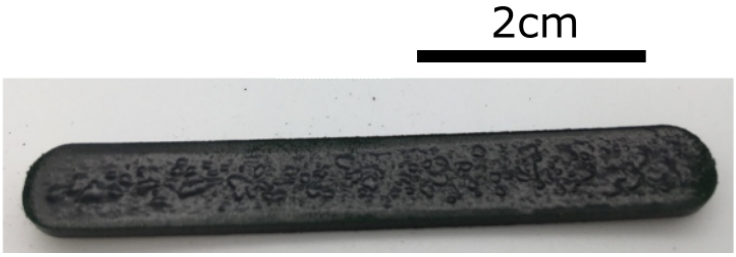

Figure 23. *Spirulina* specimen with bubbles present.

This bubbling is an indication that, while processing, the specimen can coalesce according to a mold, get disturbed by underlying moisture, and harden into a plastic layer upon cooling, similar to the behavior of many conventional plastics.

The mechanical and morphological changes in this section beg the question: what change is happening to the cells and how do they interact with each other during the hot-pressing process? The mechanisms of self-plasticization in algae cells have not been fully determined. It is known that the intracellular compounds of microalgae contain lipids that form an oil, which can be extracted for conversion into biofuels [18]. It may be the case that these oils are released from

within the cells as they are disrupted by the heat and temperature, as is the case with hot pressing for biofuel production [19]. These oils may then act as a matrix to hold the disrupted cells together, leading to a homogenous material that would be considered “plasticized”. Another hypothesis is that the hot-pressing may lead to the breaking open of sugar molecule rings within the cells, leading to the formation of short-chain polyols (similar to sorbitol) that are then able to induce plasticization in the algal cell walls. Finally, the high protein content of spirulina also allows the hypothesis that the plasticization is induced by some form of protein denaturation. In natural sources, proteins are typically folded into each other, as hydrogen bonds hold the protein structures in place. With the application of heat, the hydrogen bonds are broken, starting the process of denaturation. The protein denaturation along with the increased heat providing greater chain mobility allows the amino acid chains to entangle with each other, thus exposing new chemical groups and making the proteins more reactive while decreasing the amount of structure that the proteins provide. The entanglement allows for new interactions to occur between the protein chains, which lead to a change in bulk properties. When the material cools down after the hot-pressing is over, the chains are physically fixed in place, held together by new, possibly stronger, bonds and entangled chains [20]. More experiments are required to determine if this process is indeed occurring in hot-pressed *spirulina* cells, and if it is, whether or not it is what causes the morphological and mechanical changes observed in this study. Therefore, testing these hypotheses is beyond the scope of the present thesis and is a topic for future studies.

3.2 Mechanical and Morphological Analysis of *Spirulina*/Sorbitol

3.2.1 Mechanical Properties

The *spirulina*/sorbitol composite was produced through a method of vortex mixing and extruding the *spirulina* powder with sorbitol powder, then hot pressing and testing like the pure

spirulina specimens. As described before, the hot-pressing parameters had to be kept mild for the composite to produce testable samples.

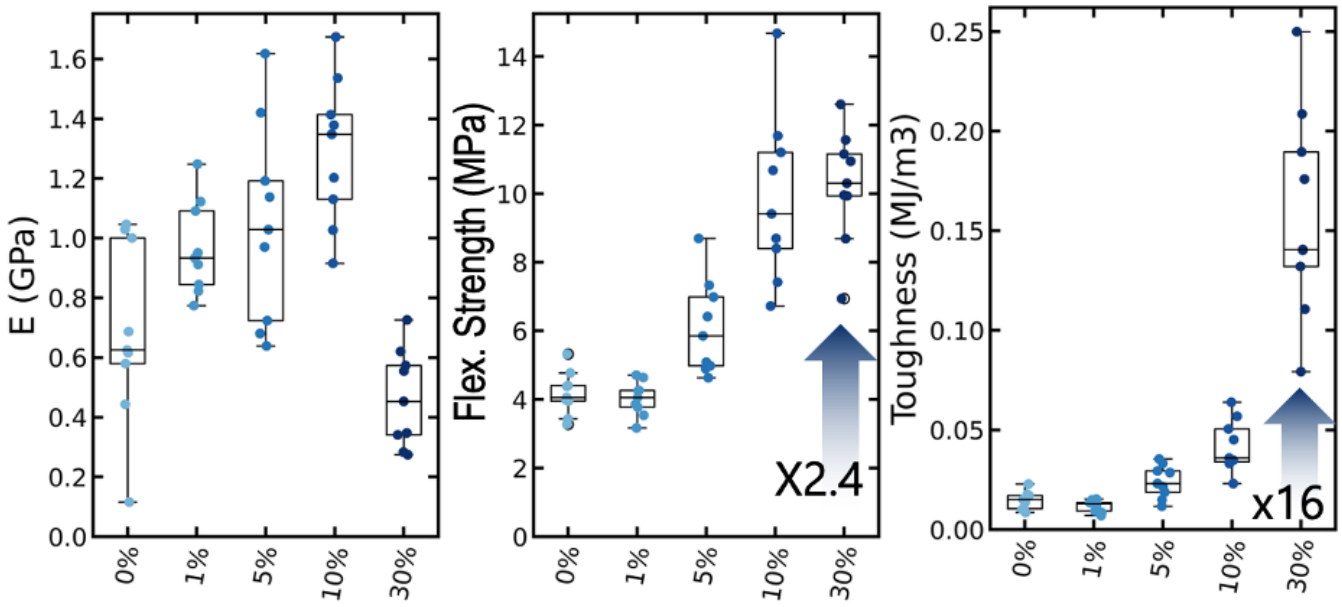

Figure 24. Box plots showing the changes in a) flexural stiffness, b) strength, and c) toughness at increasing sorbitol concentrations.

The mechanical properties of *spirulina*/sorbitol samples pressed at 80 °C/2 kN/1 min with varying concentrations of sorbitol are shown in Figure 24. Interestingly, mechanical properties do not seem to change significantly up to 10% sorbitol, with the most significant changes showing at 30% sorbitol. Higher concentrations of sorbitol were not processable because the sorbitol would flow out of the mold, pulling the *spirulina* with it and creating untestable samples. As indicated in Figures 24 and 25, the samples showed marked improvements in toughness, strength, and elongation to break, but reductions in stiffness. The strength is shown to increase by about 2.4 times (from 4.18 ± 0.60 to 10.24 ± 1.57 MPa), while the toughness increases by an impressive 16 times (from 0.01 ± 0.00 to 0.16 ± 0.05 MJ/m^3). The increases in strength indicate that the plasticizer assists in creating a uniform bulk material that is not able to be formed at the selected processing conditions without the presence of the plasticizer. This is supported by our earlier mechanical property and morphological observations that at 80 °C/2 kN the samples are loosely bonded, compacted powders rather than a fully plasticized material. The presence of the additive

above the concentration threshold of 5 wt% assists the formation of a cohesive bulk backbone in these processing conditions. The toughening and sustained extensibility before failure are known and expected effects from introducing plasticizers in bulk materials and are also observed in our case. We calculate the toughness as the area under the stress-strain curve. As shown in Figure 25, we observe that increasing amount of plasticizer leads to an increase in toughness as well as strength and strain before failure.

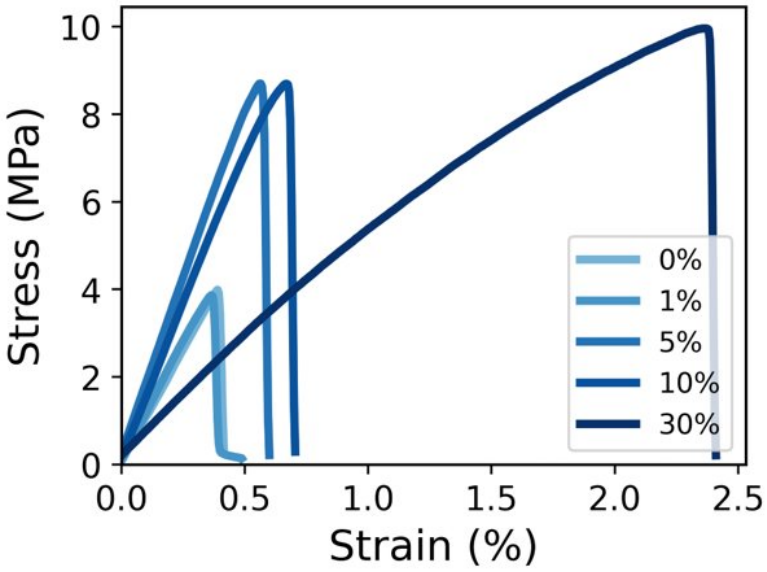

Figure 25. Representative stress-strain curves of the *spirulina*/sorbitol composites.

3.2.2 Morphological Changes

SEM imaging was used to examine the morphological changes of the *spirulina*/sorbitol samples in the same way it was used for the *spirulina* samples.

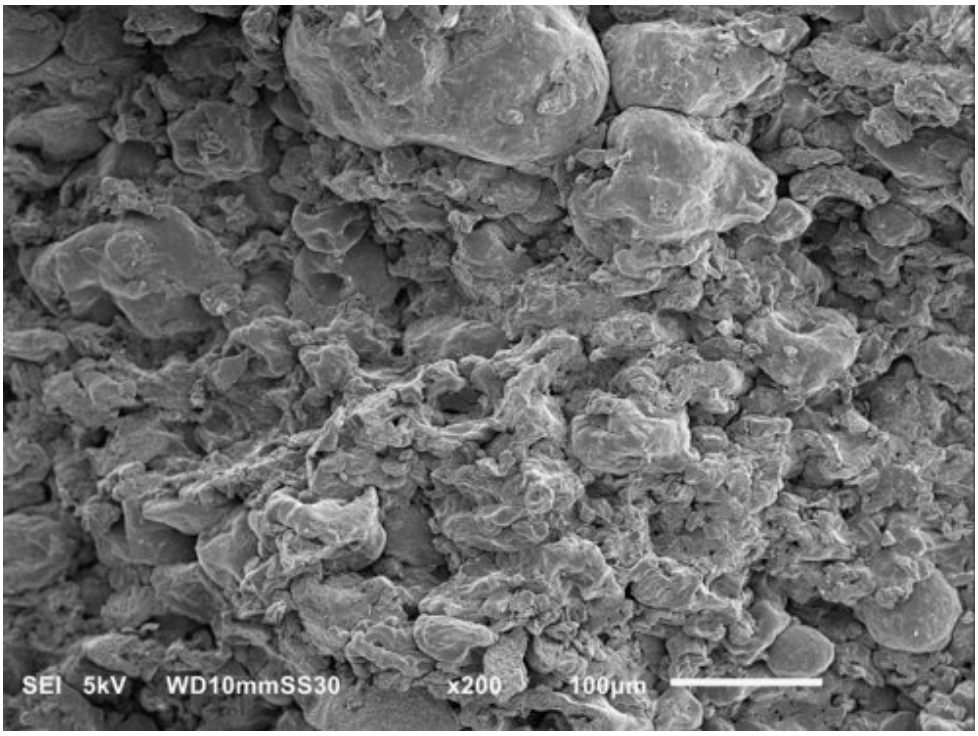

Figure 26. SEM of an unplasticized specimen used in the *spirulina*/sorbitol experiment set.

In Figure 26, the SEM image shows many clumps of *spirulina* cells, with no sorbitol added, agglomerated together in what is visually observed as a powder-packed material, with the characteristic clumps, voids, and nonuniform surface. Figure 27 shows a sample with 10% sorbitol. It has a resemblance to the unplasticized samples, with the clumps and voids, but it shows swathes of smooth surfaces. This corroborates the mechanical property results that showed lower strength and toughness for this concentration of sorbitol compared to the 10% and higher concentrations.

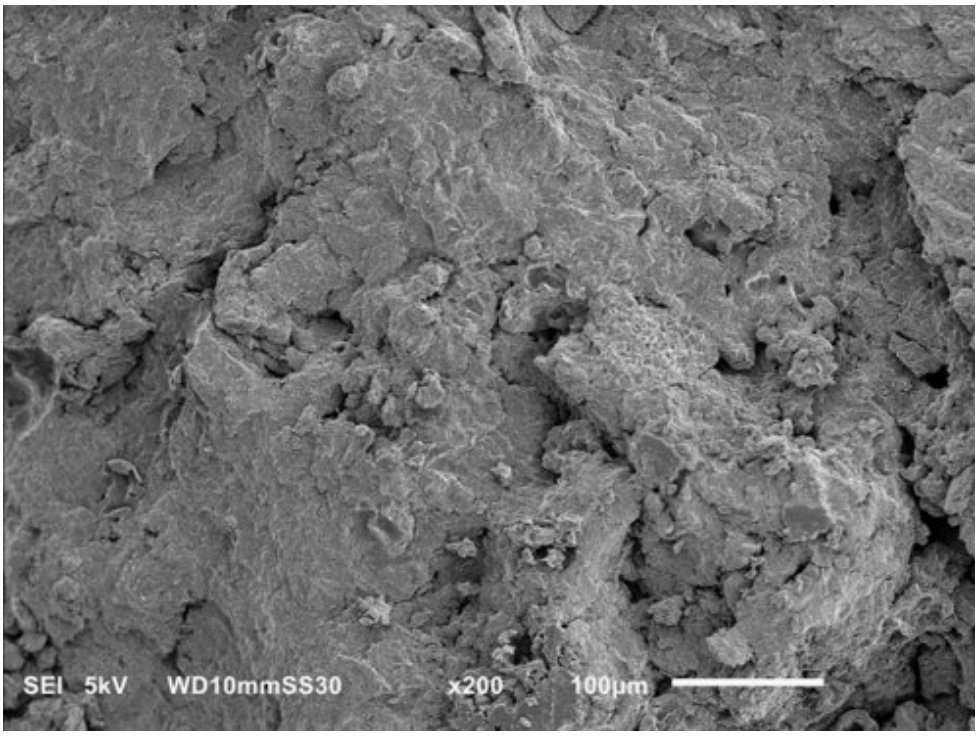

Figure 27. SEM image of a *spirulina*/sorbitol with 10 wt. % sorbitol.

The smoothness is much more extreme in Figure 28, which is of a sample with 30% sorbitol. This figure shows large swathes of smoothness with patches of rougher clumps that look more like the fully plasticized *spirulina* from Figure 20. The amount of smoothness, which may correlate to the degree of plasticization, follows the improvements in strength and toughness and the decline in elongation to break.

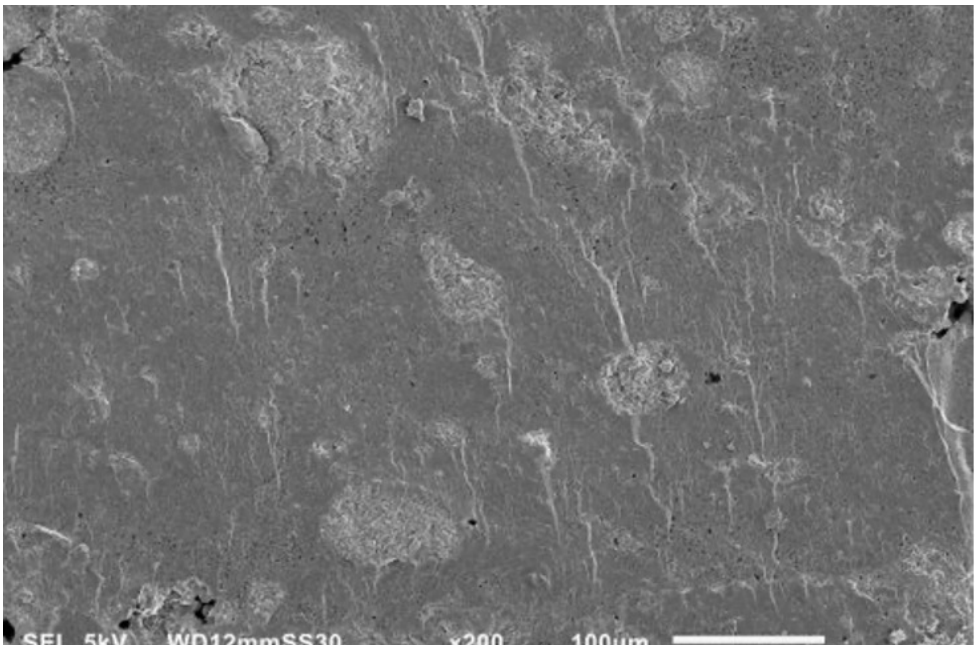

Figure 28. SEM image of a *spirulina*/sorbitol composite with 30 wt. % sorbitol.

The SEM imaging provides some insight into the mechanism of plasticization along with the change in mechanical properties. While the self-plasticization of *spirulina* appears to come from molecules within the *spirulina* cells, the sorbitol-plasticization of *spirulina* appears to come from the melting of sorbitol. Sorbitol has a melting temperature of around 90 °C, as can be seen in Figure 29. When the sorbitol is heated and pressed along with the *spirulina*, the sorbitol melts and envelopes the spirulina cells, creating a composite with sorbitol as the matrix and algal cells as the filler. This method of plasticization produces a completely different material than the plasticized *spirulina*, and it has the potential to make stronger and tougher samples if combined with the method of plasticization used for the pure *spirulina* samples.

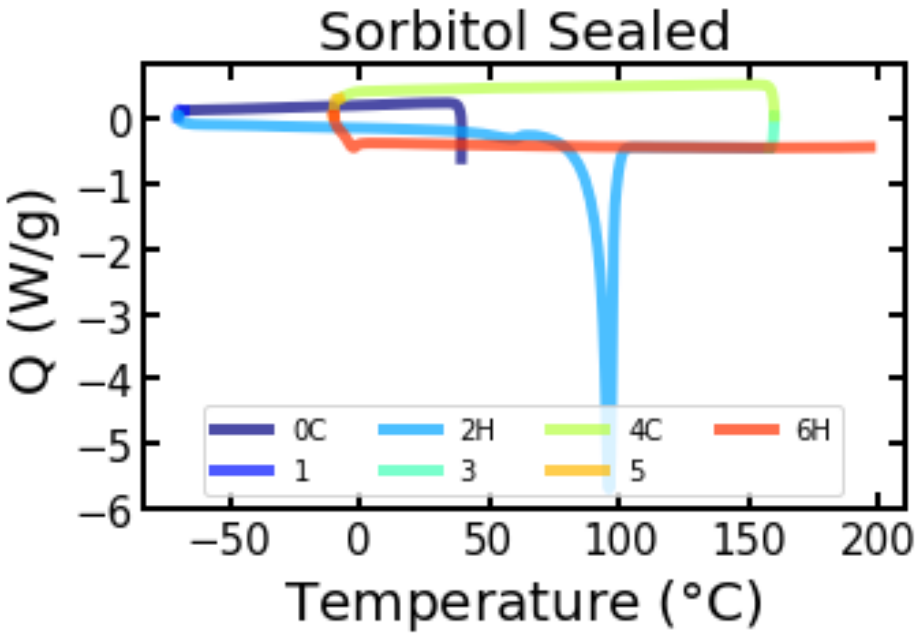

Figure 29. The DSC of pure sorbitol shows a melting temperature at 90 °C. 0C and 4C are the first and second cooling cycles, respectively, 2H and 6H are the first and second heating cycles, respectively, and 1, 3, and 5 are isothermals between cooling and heating steps.

As mentioned previously, one hypothesis for the self-plasticization is that the denaturation of proteins may lead to the exposure of new chemical groups due to the breaking of hydrogen bonds and subsequent unfolding of the amino acid chains. It is possible that the sorbitol additive reacts with the newly exposed polar groups on the unfolded proteins, allowing for a high level of incorporation of the sorbitol in the *spirulina* matrix. This may explain why sorbitol works so well as an additive with the high protein content *spirulina* cells, and how plasticization is induced in these composite materials. However, within this thesis we are not able to test and confirm this hypothesis.

3.3 Thermogravimetric Analysis

TGA was used to examine the thermal stability of our bioplastics. Figure 30 shows the thermal analysis of unpressed, powdered *spirulina* as compared to that of a pressed, well-plasticized sample. While the onset of degradation occurs at approximately the same temperature of 200 °C, an interesting difference shows up at the beginning of the graph. Water evaporation is

the expected mass loss at temperatures below 100-150 °C. Indeed, we observe a mass loss of 8% for the *spirulina* powder and 2.5% for the pressed bioplastic up to 150 °C. The powder loses significantly more mass at the beginning of the run up to approximately the onset of degradation. This indicates that the plasticization process either helps retain water within the material by turning into a homogenous object with less surface area to evaporate water, or water is being used up in the plasticization process, leaving less to be evaporated out. The first derivative of mass loss over time (DTG) shows that the main mass loss step starts at approximately 180C and shows insignificant difference between the powder and bioplastic, suggesting that the initiation of their thermal degradation coincides. Indeed, between approximately 200 and 300 C the mass loss profiles overlap. However, the following steps of thermal degradation above 300 C show distinct differences amongst the two cases. Both cases show a 3-step degradation profile, but the pressed sample has more smooth transitions between the mass loss steps. This suggest that degradation reactions happen at a different rate in the two materials, thereby confirming a major transformation in the way that the *spirulina* components are bonded after being compression molded.

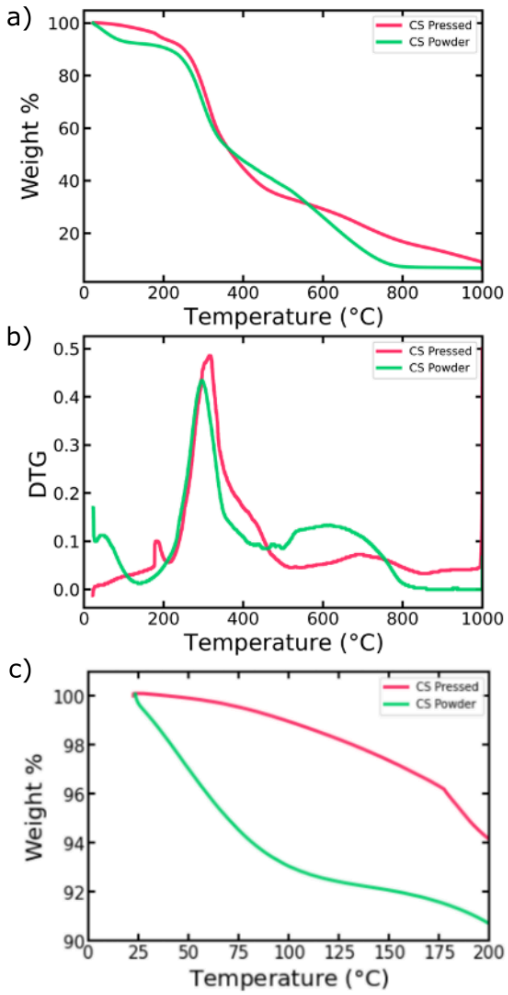

Figure 30. TGA of the original *spirulina* powder as well as a pressed *spirulina* sample.

3.4 Biodegradability

The main reason for the big research push into biomatter-based materials to replace plastics is for the inherent degradability in the final products. A biodegradation study is in progress, with six weeks of degradation complete so far. The changes in mass for the *spirulina* bioplastic, a banana peel, and a PLA sample are shown in Figure 31.

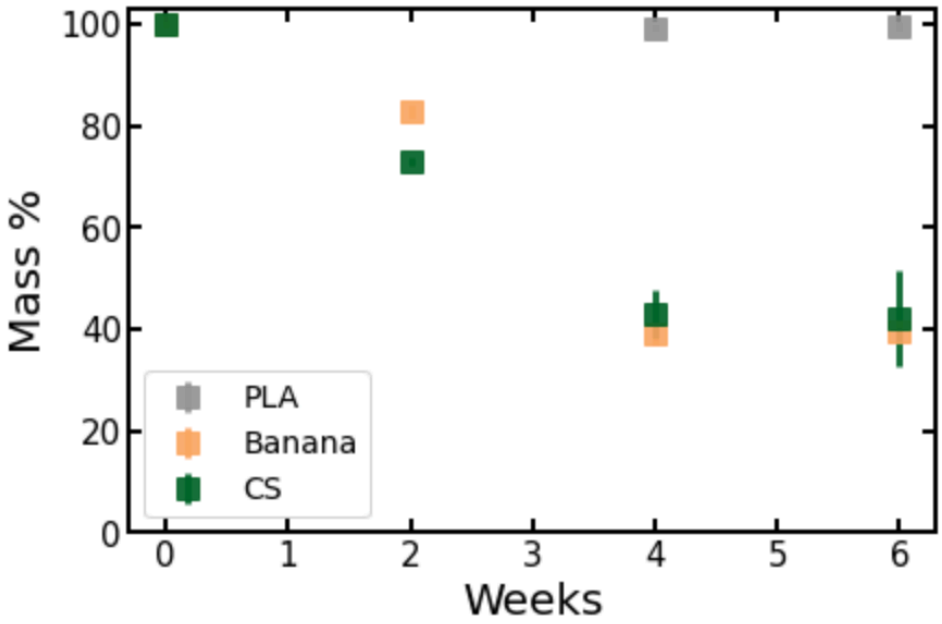

Figure 31. Biodegradation data for PLA, a banana peel, and a *spirulina* bioplastic sample.

PLA data was only recorded starting on week 4 as the mass loss was too small to be recorded during the first two weeks. However, it is noticeable that the PLA sample is hovering at over 99% of its initial weight, indicating almost no mass loss for what is one of the most commercially available compostable plastic. Meanwhile, the *spirulina* bioplastic follows the degradation of another fully natural material, a banana peel. At six weeks, the two materials had lost approximately 60% of their mass, showing that the *spirulina* bioplastics have a desirable combination of mechanical properties and degradability.

Chapter 4 – Conclusion

As part of the effort to move to more sustainable plastic materials, this study aimed to examine the relationship between processing conditions and the addition of an external plasticizer, and mechanical and morphological properties in plasticized *spirulina* algae cells. A compression molding process in which the temperature, pressure and time were varied to transform the powdered cells into hard, brittle, plastic materials. Sorbitol was mixed in with the algae cells using a twin-screw extruder to act as an external plasticizer, leading to a stronger, tougher material with higher strain to break.

We found that by holding the temperature and pressing force constant and changing the time that the material is under compression, the bending strength of the *spirulina* samples saturated at approximately 5 minutes of press time. Next, the time was held constant while a set of samples were produced according to a combination of varying temperatures and pressures. Based on the results of these tests, we found that temperature had the most significant effect on the mechanical properties, although increasing the temperature too much resulted in degradation. Pressure had an effect on mechanical properties to a point where higher pressures allowed for the cells to pack in more effectively and for the temperature to be applied to the sample more uniformly.

The effects of an external plasticizer on *spirulina* were studied by adding sorbitol to the algae cells. The two powders were vortex-mixed with varying concentrations of sorbitol, then homogenized in a twin-screw extruder. The resulting powder was pressed at conditions that lead to powder packing without plasticization in the pure *spirulina* samples. The addition of sorbitol led to increases in flexural strength and toughness of 3 and 16 times, respectively, showing that the potential for natural additives to *spirulina* is vast.

Chapter 5 – Future Work

The addition of sorbitol radically changing the mechanical properties of *spirulina*-based bioplastics makes the vast set of natural additives wide open for combining with *spirulina*. Other than short-chain sugar alcohols such as sorbitol and glycerol, nanoparticles may also be added to alter the attainable mechanical and thermal properties, along with other types of properties that nanoparticles may have an effect on. The mixing procedure, pressing conditions, and mechanical properties of the *spirulina* bioplastic with these various materials as additives would be a demanding endeavor, but it would lead to a greater understanding in how the various natural materials react with each other, and it may lead to materials with exciting mechanical and thermal properties, while maintaining biodegradability.

Besides hot pressing and extruding, more manufacturing steps can be added to the process. While that adds to the amount of energy required to produce these plastics, which affects how green the end product is, it may widen the property space available using purely natural materials. For example, adding a sonication step may reduce the clumping of algae cells, and it may break up the cells in a way that would make the plasticizers within the cells more available to the entire specimen. Humidifying the powder before pressing would increase the availability of water as a plasticizing agent, allowing for plastic specimens to be more easily produced, and perhaps with greater mechanical properties. Mixing the algae cells with water and drying the mixture or centrifuging it could potentially result in interesting materials. From preliminary studies, drying out a *spirulina*-water solution in an oven leads to glassy flakes, which would lead to a material with very different properties from those produced with the pure powder. Centrifugation of sonicated algae cells leads to the separation of smaller molecules in the cells from the larger molecules, and the study of each of these sets of molecules may lead to insight on why

plasticization occurs in these materials and how to tune the composition of the pressed powder to achieve desired mechanical properties.

Finally, a study into the actual plasticization mechanism needs to be conducted to elucidate the behavior of proteins, fats, and other functional units within *spirulina* cells as they undergo changes in temperature and pressure. As the method of plasticization is unknown, an examination of protein denaturation in algae could shed light on how best to take advantage of this self-plasticizing ability, as well as how best to incorporate additives to tune the mechanical properties even further.

Chapter 6 – References

1. Mohanty, A. *et al*. Composites from renewable and sustainable resources: Challenges and innovations. *Science* **362**, 6414, 536-542 (2018).
2. Rochman, C. *et al.* Classify plastic waste as hazardous. *Nature* **494**, 169-171 (2013).
3. Leslie, H. *et al.* Discovery and quantification of plastic particle pollution in human blood. *Environment International* **163**, 107199 (2022)
4. Reddy, M. *et al.* Biobased plastics and bionanocomposites: Current status and future opportunities. *Progress in Polymer Science* **38**, 10-11, 1653-1689 (2013).
5. Noreen, A. *et al.* A critical review of algal biomass: A versatile platform of bio-based polyesters from renewable resources. *International Journal of Biological Macromolecules* **86**, 937-949 (2016).
6. Jem, K. *et al.* The development and challenges of poly (lactic acid) and poly (glycolic acid). *Advanced Industrial and Engineering Polymer Research* **3**, 2, 60-70 (2020).
7. Moon, R. *et al.* Cellulose nanomaterials review: structure, properties and nanocomposites. *Chemical Society Reviews* **7**, (2013).
8. Xia, Q. *et al.* A strong, biodegradable and recyclable lignocellulosic bioplastic. *Nature Sustainability* **4**, 627-635 (2021).
9. Fredricks, J. *et al.* The effects of temperature, pressure, and time on lignin incorporation in bacterial cellulose materials. *MRS Communications* (2022)
10. Tedeschi, G. *et al.* Multifunctional bioplastics inspired by wood composition: effect of hydrolyzed lignin addition to xylan-cellulose matrices. *Biomacromolecules* **21**, 2, 910-920 (2020)
11. Sakakibara, K. *et al.* Preparation of high-performance polyethylene composite materials reinforced with cellulose nanofiber: simultaneous nanofibrillation of wood pulp fibers

during melt-compounding using urea and diblock copolymer dispersant. *ACS Applied Polymer Materials* **1**, 2, 178-187 (2019)

12. Zhang, C. *et al.* Progress and perspective on algal plastics – A critical review. *Bioresource Technology* **289**, 121700 (2019).
13. Mathiot, C. *et al.* Microalgae starch-based bioplastics: Screening of ten strains and plasticization of unfractionated microalgae by extrusion. *Carbohydrate Polymers* **208**, 142-151 (2019).
14. Zeller, M. *et al.* Bioplastics and their thermoplastic blends from *Spirulina* and *Chlorella* microalgae. *Journal of Applied Polymer Science* **130**, 5, 3263-3275 (2013)
15. Dianursanti *et al.* The effect of compatibilizer and addition on *Chlorella vulgaris* microalgae utilization as a mixture for bioplastic. *E3S Web Conf.* **67**, (2018)
16. Otsuki, T. *et al.* Synthesis and tensile properties of a novel composite of *Chlorella* and polyethylene. *Journal of Applied Polymer Science* **92**, 2, 812-816 (2004).
17. Matveev, Y. *et al.* The plasticizing effect of water on proteins, polysaccharides, and their mixtures. Glassy state of biopolymers, food and seeds. *Food Hydrocolloids* **14**, 5, 425-437 (2000).
18. Show, K. *et al.* Microalgal drying and cell disruption – Recent advances. *Bioresource Technology* **184**, 258-266 (2015).
19. Vieira, M. *et al.* Natural-based plasticizers and biopolymer films: A review. *European Polymer Journal* **47**, 3, 254-263 (2011).
20. De Graaf, L. Denaturation of proteins from a non-food perspective. *Journal of Biotechnology* **79**, 3, 299-306 (2000).